OncoTargets and Therapy Dovepress

Open Access Full Text Article ORIGINAL RESEARCH

Prognostic Value of miR-10a-3p in Non-Small Cell Lung Cancer Patients

Julija Simiene[1,2], Linas Kunigenas[1,2], Rimvile Prokarenkaite[1,2], Daiva Dabkeviciene[2,3], Egle Strainiene[1,4], Vaidotas Stankevicius[1,5], Saulius Cicenas[6], Kestutis Suziedelis[1,2]

[1]Laboratory of Molecular Oncology, National Cancer Institute, Vilnius, LT-08406, Lithuania; [2]Institute of Biosciences, Life Sciences Center, Vilnius University, Vilnius, LT-10223, Lithuania; [3]Biobank, National Cancer Institute, Vilnius, LT-08406, Lithuania; [4]Department of Chemistry and Bioengineering, Vilnius Gediminas Technical University, Vilnius, LT-10223, Lithuania; [5]Institute of Biotechnology, Life Sciences Center, Vilnius University, Vilnius, LT-10223, Lithuania; [6]Department of Thoracic Surgery and Oncology, National Cancer Institute, Vilnius, LT-08406, Lithuania

Correspondence: Julija Simiene, Laboratory of Molecular Oncology, National Cancer Institute, Vilnius, LT-08406, Lithuania, Tel +37052190907, Email julija.simiene@nvi.lt

Purpose: Poor lung cancer patients' outcomes and survival rates demand the discovery of new biomarkers for the specific, significant, and less invasive detection of non-small cell lung cancer (NSCLC) progression. The present study aimed to investigate the potential of miRNA expression as biomarkers in NSCLC utilizing a preclinical cell culture setup based on screening of miRNAs in NSCLC cells grown in 3D cell culture.

Patients and Methods: The study was performed using lung cancer cell lines, varying in different levels of aggressiveness: NCI-H1299, A549, Calu-1, and NCI-H23, as well as noncancerous bronchial epithelial cell line HBEC3, which were grown in 3D cell culture. Total RNA from all cell lines was extracted and small RNA libraries were prepared and sequenced using the Illumina NGS platform. The expression of 8 differentially expressed miRNAs was further validated in 89 paired tissue specimens and plasma samples obtained from NSCLC patients. Statistical analysis was performed to determine whether miRNA expression and clinico-pathological characteristics of NSCLC patients could be considered as independent factors significantly influencing PFS or OS.

Results: Differentially expressed miRNAs, including let-7d-3p, miR-10a-3p, miR-28-3p, miR-28-5p, miR-100-3p, miR-182-5p, miR-190a-5p, and miR-340-5p, were identified through next-generation sequencing in NSCLC cell lines with varying levels of aggressiveness. Validation of patient samples, including tumor and plasma specimens, revealed that out of the 8 investigated miRNAs, only plasma miR-10a-3p showed a significant increase, which was associated with significantly extended progression-free survival (PFS) (p=0.009). Furthermore, miR-10a-3p in plasma emerged as a statistically significant prognostic variable for NSCLC patients' PFS (HR: 0.5, 95% CI: 0.3–0.9, p=0.029).

Conclusion: Our findings of screening miRNA expression patterns in NSCLC cells grown in 3D cell culture indicated that the expression level of circulating miR-10a-3p has the potential as a novel non-invasive biomarker to reflect the short-term prognosis of NSCLC patients.

Keywords: NSCLC, miRNAs, non-invasive clinical biomarkers, 3D cell culture, survival

Introduction

Lung cancer is currently the most diagnosed cancer type among both men and women and is the leading cause of cancer-related deaths worldwide.[1] Despite the progress made in diagnostics and treatment, more than 75% of lung cancer cases are diagnosed in advanced or metastatic stages.[2] Non-small cell lung cancer, accounting for 85%, represents the most common type of lung cancer. Due to its rapid invasion and metastasis formation, the overall 5-year survival rate after initial diagnosis is lower than 15%.[3] Therefore, investigating the molecular mechanisms involved in lung cancer carcinogenesis and progression is crucial for the development of new effective therapeutic targets.[4]

Poor NSCLC patients' outcomes urgently demand the discovery of new biomarkers for the specific and less invasive detection of lung cancer progression. MicroRNAs (miRNAs) seem to join the pieces of this puzzle and may help to find out the biology of cancer cell invasiveness and migration processes.[5] miRNAs are small non-coding ~22nt length RNAs that inhibit

Received: 26 April 2024
Accepted: 20 September 2024
Published: 14 November 2024

mRNA translation or negatively regulate mRNA stability by binding to target mRNAs' 3′-untranslated region (3′-UTR).[6] Accumulating evidence shows that miRNAs may be associated with NSCLC invasion, metastasis, and angiogenesis, as well as playing a critical role in either the progression or prognosis of lung cancer.[7,8] Therefore, determining the regulatory functions of miRNAs and their undergoing mechanism is important for improving our knowledge of NSCLC development and progression.[9] Previous studies in lung cancer patients show promising results for microRNA integration in clinical settings. A combination of miR-21, miR-210 and miR-486-5p were shown to successfully differentiate patients with benign or malignant pulmonary nodules from blood plasma.[10] This same miRNA panel later demonstrated diagnostic potential in differentiating NSCLC from healthy individuals using blood plasma.[11] miR-205 expression assay has been shown to identify squamous cell carcinoma using formalin fixed tissue samples.[12] Serum miRNAs miR-486, miR-30d, miR-1 and miR-499 have been shown to work as predictors of overall survival.[13] Even less invasive approaches are possible using miRNAs. miR-21 in sputum has been shown to diagnose NSCLC.[14] A combination of miR-205, miR-210 and miR-708 in sputum has been shown to diagnose squamous cell carcinoma even at early stages of the disease.[15] Another study identified sputum miR-31-5p and miR-210-3p as capable predictors of NSCLC.[16]

NSCLC cell lines play a crucial role in enhancing our understanding of the fundamental molecular principles underlying lung cancer invasiveness and the potential for metastasis formation, making them essential tools for preclinical research.[17] For instance, H1299, also known as NCI-H1299 or CRL-5803, is a human non-small cell lung carcinoma cell line derived from lymph nodes. According to the study results, this cell line exhibits the most aggressive features.[18] Like other immortalized cell lines, H1299 cells can divide indefinitely and are characterized by a lack of expression of the p53 protein due to a homozygous partial deletion of the gene.[19] Other highly aggressive cell lines include Calu-1, an epidermoid lung carcinoma cell line with the Ras (K-ras) oncogene, and A549, adenocarcinoma human alveolar basal epithelial cells.[20,21] The H23 cell line is characterized as a least aggressive non-small cell lung cancer cell line with the K-ras 12 mutation and a p53 mutation in codon 246 (ATC → ATG, isoleucine → methionine).[18] Thus, all these cell lines are extensively used in NSCLC research due to their representation of different NSCLC subtypes, including adenocarcinoma and squamous cell carcinoma. These well-characterized cell lines offer various genetic backgrounds and are valuable for investigating cancer mechanisms and testing new therapies. A further application of cancer cell line models with varying levels of aggressiveness could be exploited to identify important biomarkers related to NSCLC invasiveness and progression.[22]

While two-dimensional (2D) cell cultures, involving monolayers on flat surfaces, have their utility, it does not faithfully replicate the in vivo environment as effectively as three-dimensional (3D) cell cultures do. Numerous studies have demonstrated that gene expression profiles in multicellular spheroid 3D models closely resemble those found in tumors in vivo.[23] Accordingly, 3D cancer models hold significant biological relevance for preclinical testing of tumor development and progression.[24] Given that the identification of novel biomarkers necessitates the use of hundreds of high-quality patient samples, which can impede the validation of reproducible, specific, and sensitive biomarkers, this suggests the utilization of NSCLC 3D cell culture models depicting a range of cancer cell aggressiveness could be applied for further discovery of new clinically relevant biomarkers.

The present study aims to investigate the potential of miRNA expression as biomarkers in NSCLC utilizing a preclinical cell culture setup based on screening of miRNAs in NSCLC cells grown in 3D cell culture. For this purpose, we employed human bronchial epithelial cell line HBEC3, as well as human lung cancer cell lines NCI-H1299, A549, Calu-1, and NCI-H23 cells, and grown them in 3D cell culture for 6 days. Illumina® NGS analysis revealed eight miRNAs were commonly expressed in NSCLC with the highest aggressiveness status. The expression analysis of selected miRNAs in 89 paired tumor tissue specimens and plasma samples from NSCLC patients revealed that, out of the 8 miRNAs tested after cell sequencing, only the circulating miR-10a-3p can be evaluated as a novel non-invasive biomarker for NSCLC outcomes. This suggests that using 3D cell cultures is a highly valuable tool for biomarker discovery. Additionally, determining miRNA expression in both tumor tissue and serum samples is crucial. Serum samples, in particular, are important because they offer a less invasive, less expensive, and less harmful approach for the patient. Overall, we show that the screening of miRNA profiles determined using cancer cells lines growing them in 3D cell cultures could have potential diagnostic applications in assessing patients with NSCLC.

Materials and Methods

Cell Culture Maintenance

The human bronchial epithelial cell HBEC3 (ATCC No. CRL-4051) and human lung cancer cell lines NCI-H1299 (ATCC No. CRL-5803), A549 (ATCC No. CCL-185), Calu-1 (ATCC No. HTB-54) and NCI-H23 (ATCC No. CRL-5800) were purchased from American Type Culture Collection (ATCC, USA). HBEC cells were grown in an Airway Epithelial Cell Basal Medium (ATCC PCS-300-030) supplemented with a Bronchial Epithelial Cell Growth Kit (ATCC PCS-300-040) containing 1% penicillin/streptomycin mix. NCI-H1299 and NCI-H23 cells were grown in ATCC-formulated RPMI-1640 Medium (ATCC 30-2020) containing 10% fetal bovine serum and 1% penicillin/streptomycin mix. A549 (ATCC No. CRM-CCL-185) cells were grown in ATCC-formulated F-12K medium (ATCC No. 30-2004) containing 10% fetal bovine serum and 1% penicillin/streptomycin mix. Calu-1 cells were grown in ATCC-formulated McCoy's 5a Medium (ATCC 30-2007) containing 10% fetal bovine serum and 1% penicillin/streptomycin mix. Cells were cultured in 25 cm^2 plastic cell culture flasks incubated at 37°C and 5% CO_2. The medium was renewed every 2–3 days. After the monolayer of cells became 80% confluent, sub-cultivation was carried out using 0.05% Trypsin-EDTA in DPBS (1x) (Capricorn Scientific GmbH, Germany).

3D Cell Culture Model

HBEC3, NCI-H1299, A549, Calu-1, and NCI-H23 cell lines were cultured in 3D cell cultures for a duration of six days. To achieve this, 5×10^3 cells of HBEC3, NCI-H1299, and A549, and 4×10^3 cells of Calu-1 and NCI-H23 were suspended in 200 µL of cell culture medium and seeded into individual wells of 96 round-bottom plates previously coated with a 1% agarose in water gel. The plates were subsequently centrifuged at 750 × g for 15 minutes. Imaging of the cells was performed every two days using an inverted optical microscope Eclipse TS100 and a digital camera DS-Fi2 (Nikon, Japan). The size of the multicellular spheroids was determined using SpheroidSizer 1.0.[25] Each experiment was conducted independently and repeated a minimum of three times.

Patients and Methods

The study was conducted using a total of 89 paired tissue specimens, which included both NSCLC tumors and their adjacent noncancerous tissues. Additionally, 89 plasma samples were collected from both NSCLC patients and healthy individuals to serve as normal controls. All samples were obtained from patients who had not undergone pre-operative chemotherapy or radiotherapy. The surgical treatment, which included either segmentectomy, lobectomy, or pneumonectomy, was performed at the Department of Thoracic Surgery and Oncology of the National Cancer Institute in Vilnius, Lithuania, and was determined individually based on the specific location and extent of the cancerous process for each patient. All procedures were performed in compliance with relevant laws and institutional guidelines and have been approved by the Lithuanian Bioethics Committee (Approval No. 158200-05-455-141), and all patients provided written informed consent before sample collection. Following surgical treatment, all patients received four cycles of adjuvant combination therapy every three weeks, involving a platinum-based drug (cisplatin or carboplatin, administered intravenously at a dose of 80 mg/m^2 and 5 AUC, respectively) and etoposide (administered intravenously at a dose of 120 mg/m^2) for further treatment. The adjuvant chemotherapy regimen commenced 3–4 weeks after the completion of surgical treatment. The median age of patients enrolled in the study was 68 years, including those at disease stages IB-IV. To improve the accuracy of statistical calculations, the subjects were subsequently divided into two groups: earlier stages (I–II) and later stages (III–IV), with both groups treated according to standard protocols. The median follow-up period for the patients was 49 months, with a range spanning from 1 to 98 months. Regarding treatment response, 49.4% (n=44) of patients exhibited a positive response (stable disease), while 50.6% (n=45) experienced disease progression. The clinicopathological characteristics of the study cohort are summarized in Table 1.

miRNA Isolation

To extract miRNA, the miRNeasy Mini Kit (Qiagen, Germany) was used according to the manufacturer's instructions on all cell lines grown in 3D culture for six days. Upon resection, lung cancer tumors and their matched noncancerous

Table 1 Clinicopathological Characteristics of NSCLC Patients

Characteristic	Cases, n (%)
Age	
≤ 68	47 (52.8)
> 68	42 (47.2)
Gender	
Female	12 (13.5)
Male	77 (86.5)
Smoking status	
Never	35 (39.3)
Smoking	54 (60.7)
Pathological stage	
Stage I/II	65 (73.0)
Stage III/IV	24 (27.0)
Lymph node status	
N0	49 (55.1)
N1	23 (25.8)
N2	17 (19.1)
Tumor differentiation grade	
G1	5 (5.6)
G2	30 (33.7)
G3	54 (60.7)
Tumor histology	
ADC	45 (50.6)
SCC	44 (49.4)
Treatment response	
Stable disease	44 (49.4)
Progression	45 (50.6)

Abbreviations: N0, no regional lymph nodes involvement; N1, involvement of ipsilateral peribronchial and/or ipsilateral hilar lymph nodes (includes direct extension to intrapulmonary nodes); N2, involvement of the ipsilateral mediastinal and/or subcarinal lymph nodes; G1, well differentiated; G2, moderately differentiated; G3, poorly differentiated; ADC, adenocarcinoma; SCC, squamous cell carcinoma.

tissues underwent histological examination by a pathologist before being promptly frozen in liquid nitrogen and stored at −150 °C to ensure their preservation. Plasma samples from NSCLC patients and normal control samples were frozen and stored at −70 °C. Extraction of total RNA from tumor and adjacent normal tissues was carried out using the mirVanaTM miRNA isolation kit (Ambion, USA) following the manufacturer's protocol. Similarly, miRNAs from NSCLC plasma and control samples were extracted using the miRNeasy Serum/Plasma Kit (Qiagen, Germany). The quantity and quality of RNA were evaluated using a Nanodrop instrument (ThermoFisher Scientific, USA). Bioanalyzer 2100 (Agilent, Santa Clara, California, USA) was used for subsequent RNA integrity assessment based on the evaluation of 28S and 18S ribosomal subunit peaks in the electropherogram.

miRNA Sequencing and Data Processing

Using the QIAseq miRNA Library Kit (Qiagen, Germany) as per the manufacturer's instructions, small RNA libraries were prepared. NextSeq 550 (Illumina, USA) was used for high-throughput sequencing. Finally, the quality of Next Generation Sequencing (NGS) data of small RNA was evaluated using FastQC v.0.11.5, as previously described.[26] 3′ adapter sequences were removed using Cutadapt v.1.15 tool.[27] Reads shorter than 15 nucleotides and less than quality score 25 were excluded from further analysis. The remaining reads were aligned to the human genome GRCh38p12 using a short-read aligner Bowtie2.[28] Genome-mapped sequences were further aligned to the annotated mature miRNA sequences from the miRBase v22.1 data repository.[29]

To evaluate differences of miRNA expression between cell lines cultivated as multicellular spheroids, the abundance of mapped mature miRNAs was measured, and counts were submitted for differential expression analysis using the edgeR application.[30] Mature miRNA counts were normalized using the intrinsic TMM method. Statistical analysis was performed using Fisher's exact test. To reduce false discovery rate, the Benjamini – Hochberg method was used to adjust p values. miRNAs with relative expression of 2-fold, adjusted p value less than 0.05, and at least 10 reads per million of mapped transcripts were considered significantly differentially expressed. NGS data were submitted to the GEO database and are available with accession number GSE245576.

miRNA Target Analysis

To assess the role of differentially expressed miRNAs Diana Lab Tools was used to extract target genes from the target database TarBase v8.[31] WebGestalt 2019 online toolkit was used to perform KEGG pathway enrichment analysis of miRNA target genes.[32] The weighted set cover function was used to reduce redundancy. Pathways with at least 5 genes assigned and a false discovery rate lower than 0.05 were considered significantly enriched.

Quantitative Real-Time PCR

For miRNA sequencing data validation, the expression of miRNAs in tissue and plasma samples was quantified by RT-qPCR method. cDNA synthesis was performed using Revert Aid RT Kit and stem-loop RT primer for tissue miRNA samples (ThermoFisher Scientific, USA) or using TaqMan MicroRNA Reverse Transcription Kit (Applied Biosystems, USA) for plasma miRNA. RT-qPCR was performed using Realplex4 Mastercycler thermocycler (Eppendorf, Hamburg, Germany). Evaluation of miRNA expression in tissue was performed using Luminaris HiGreen qPCR Master Mix (ThermoFisher Scientific, USA) or implementing TaqMan MicroRNA Assays with miRNA-specific primers (Applied Biosystems, USA) for plasma miRNA samples. In this study, all experimental procedures were conducted meticulously according to the manufacturer's instructions to ensure accuracy of results. The expression levels of miRNA were analyzed in relation to the expression of the housekeeping gene RNU6B. To minimize the chances of error, each sample was assessed in triplicate, and the $2^{-\Delta Ct}$ method was used to calculate the results.[33]

Statistical Analysis

The statistical analysis was performed using either the data analysis software package SPSS 20.0 (IBM Corp). or GraphPad v8.0 (GraphPad Software, Inc.). The normality of the data was checked using the Shapiro–Wilk *W*-test. Wilcoxon (for paired samples) and Mann–Whitney (for unpaired samples) tests were used to analyze the differences in expression levels between tumor and adjacent normal tissue. Based on gene (let-7d-3p, miR-10a-3p, miR-28-3p, miR-28-5p, miR-100-3p, miR-182-5p, miR-190a-5p, miR-340-5p) median expression (cut-off value), all patients were divided into two groups: low expression group (samples with less than median expression level) and high expression group (samples with above median value). The distribution of cases with low or high miRNA levels in tumor and plasma samples was analyzed using a two-sided Chi-square test or Fisher's exact test, according to the demographic and clinicopathological characteristics of the patients. The overall survival (OS) and progression-free survival (PFS) were evaluated using Kaplan-Meier analysis and Log rank test. Univariate and multivariate Cox regression analysis was used to identify independent factors determining PFS or OS. Differences were considered statistically significant when the p-value was less than 0.05.

Results

miRNA Expression Profiling in NSCLC Cells

To reveal miRNA expression patterns in lung cancer cells, miRNA sequencing was conducted on five lung cell lines cultured as multicellular spheroids. For this study we selected 4 cancer cell lines of putatively varying degrees of aggressiveness and 1 normal lung cell line to serve as baseline for miRNA expression levels. miRNA sequencing analysis revealed significant expression differences between cell lines (Figure 1A). In the least aggressive lung cancer cell line H23 272 miRNAs were differentially expressed, Calu-1 – 139, A549 – 207, and most aggressive H1299 – 252 compared to normal lung cell line HBEC. Except for Calu-1 (46%) all other cell lines displayed dominant miRNA expression upregulation (65.8–67.9% of differentially expressed miRNAs were upregulated). The majority of differentially expressed miRNAs were shared between at least two cell lines. Uniquely expressed miRNAs made up 61 (22.4%), 9 (6.5%), 36 (14.3%), and 24 (11.6%) of all differentially expressed miRNAs for H23, Calu-1, H1299, and A549 cell lines respectively (Figure 1A). The analysis revealed that there were 8 commonly deregulated miRNAs in the more aggressive Calu-1, H1299, and A549 cells, therefore we selected them to investigate further (Figure 1B).

In accordance with global miRNA expression changes, 5 of 8 common differentially expressed miRNAs were overexpressed in all three aggressive cell lines (miR-10a-3p, miR-100-3p, miR-190a-5p, miR-28-5p, miR-28-3p, and miR-182-5p). miR-182-5p were exclusively downregulated in all aggressive cell lines, whereas the direction of regulation of miR-340-5p and let-7d-3p in Calu-1 opposed that of H1299 and A549.

In silico analysis of potential miRNA target genes was performed to gain a better understanding of the biological pathways of differentially expressed miRNAs (Table 2). Target analysis revealed genes implicated in several KEGG pathways indicating that adherens junction, cell cycle, FoxO signaling pathway, and cellular senescence were the most enriched categories showing almost twice gene enrichment than random chance. Other significantly enriched KEGG pathways were implicated in protein processing and degradation, infectious diseases, cancer, and endocytosis.

miRNAs Expression in NSCLC Patient Samples

Since in vitro determined common miRNAs could be potentially associated with lung tumor aggressiveness as well, we selected these miRNAs (let-7d-3p, miR-10a-3p, miR-28-3p, miR-28-5p, miR-100-3p, miR-182-5p, miR-190a-5p, miR-340-5p) to further investigate whether it could provide valuable insights into cancer progression and prognosis in NSCLC patients as potential biomarkers in tumor tissue and plasma samples by qRT-PCR.

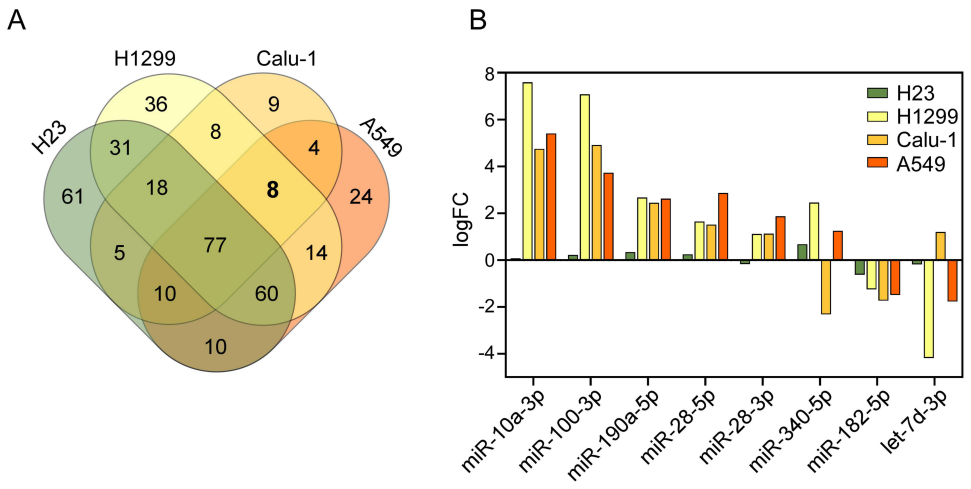

Figure 1 miRNA expression pattern in lung cancer cell lines in contrast to normal lung cell line. (**A**) Venn diagram demonstrating counts of statistically significant differentially expressed miRNAs in H23, H1299, Calu-1, and A549 (>2 fold-change, FDR<0.05, at least 10 mapped reads per million transcripts in miRNA library) compared to normal lung cell line HBEC. The bold text represents 8 commonly deregulated miRNAs in the more aggressive Calu-1, H1299, and A549 cells. (**B**) Expression pattern of miRNAs differentially expressed in lung cancer H23, H1299, Calu-1, and A549.

Table 2 KEGG Pathways of miRNA Target Analysis

Description	Genes	Ratio	FDR
Adherens junction	38	2.2616	2.10E-06
Cell cycle	58	2.0043	4.49E-07
FoxO signaling pathway	61	1.9803	4.49E-07
Cellular senescence	73	1.9551	1.04E-07
Ubiquitin mediated proteolysis	55	1.7203	9.05E-05
Protein processing in endoplasmic reticulum	66	1.7141	1.80E-05
Human T-cell leukemia virus 1 infection	99	1.6636	7.22E-07
Viral carcinogenesis	74	1.5776	1.10E-04
Pathways in cancer	179	1.4583	4.49E-07
Endocytosis	78	1.3698	5.68E-03

Abbreviations: FDR, false discovery rate; the enrichment ratio is computed by dividing a number of genes mapped to a specific pathway by an expected number of genes to map by random chance. Expected values are calculated by multiplying proportional size of the pathway in relation to all annotated genes by the number of genes present in the input.

miRNA expression analysis revealed that the expression level of let-7d-3p in NSCLC tissue was significantly increased compared to normal tissue ($p < 0.001$) (Figure 2A). Although Figure 2B indicated that the expression levels of miR-10a-3p is slightly higher in normal samples, there was no statistically significant difference in miR-10a-3p expression between cancer and normal specimens, in both tissue and plasma samples. Whereas, the expression level of miR-28-3p, miR-28-5p, miR-100-3p, miR-182-5p, miR-190a-5p, and miR-340-5p was significantly higher in normal samples compared to NSCLC tissue and plasma samples (Figure 2C–H). Overall, these findings underscore the potential importance of these miRNAs in the context of NSCLC pathogenesis and may warrant further investigation for their diagnostic or therapeutic implications in lung cancer.

miRNA Expression Levels in Relation to the Clinicopathological Characteristics

We investigated the distribution of low and high expression levels of let-7d-3p, miR-10a-3p, miR-28-3p, miR-28-5p, miR-100-3p, miR-182-5p, miR-190a-5p, and miR-340-5p in both tumor tissue and plasma samples among NSCLC patients. This analysis considered demographic and clinicopathological characteristics, using two-sided Chi-square or Fisher's exact tests for evaluation (Tables S1–S4). Changes in miR-100-3p expression in tumor tissue were significantly associated with tumor histology (p=0.034), while miR-100-3p expression in plasma was significantly associated with patients' smoking status (p=0.009). Moreover, low miR-10a-3p expression in NSCLC plasma samples showed a significant relationship with disease progression (p=0.020). The distribution between let-7d-3p, miR-10a-3p, miR-28-3p, miR-28-5p, miR-100-3p, miR-182-5p, miR-190a-5p, and miR-340-5p expression in tumor tissue as well as plasma samples and demographic, clinicopathological characteristics of the patients are presented in Tables S1–S4.

Association of miRNAs Expression Levels and NSCLC Patient Survival Rates

The prognostic value of let-7d-3p, miR-10a-3p, miR-28-3p, miR-28-5p, miR-100-3p, miR-182-5p, miR-190a-5p, and miR-340-5p expression in NSCLC tumor tissues and plasma samples was investigated. The median time of overall survival (OS) and progression-free survival (PFS) was established and compared to each group using Kaplan-Meier analysis.

The mean OS for all NSCLC patients was 51.4 months (95% CI: 44.2–58.6), and when stratified by high expression levels of specific miRNAs in tumor tissue and plasma, the OS rates varied as follows: for let-7d-3p, 49.2 months (95% CI: 39.2–59.3) in tumor and 52.4 months (95% CI: 43.3–61.6) in plasma; for miR-10a-3p, 51.5 months (95% CI:

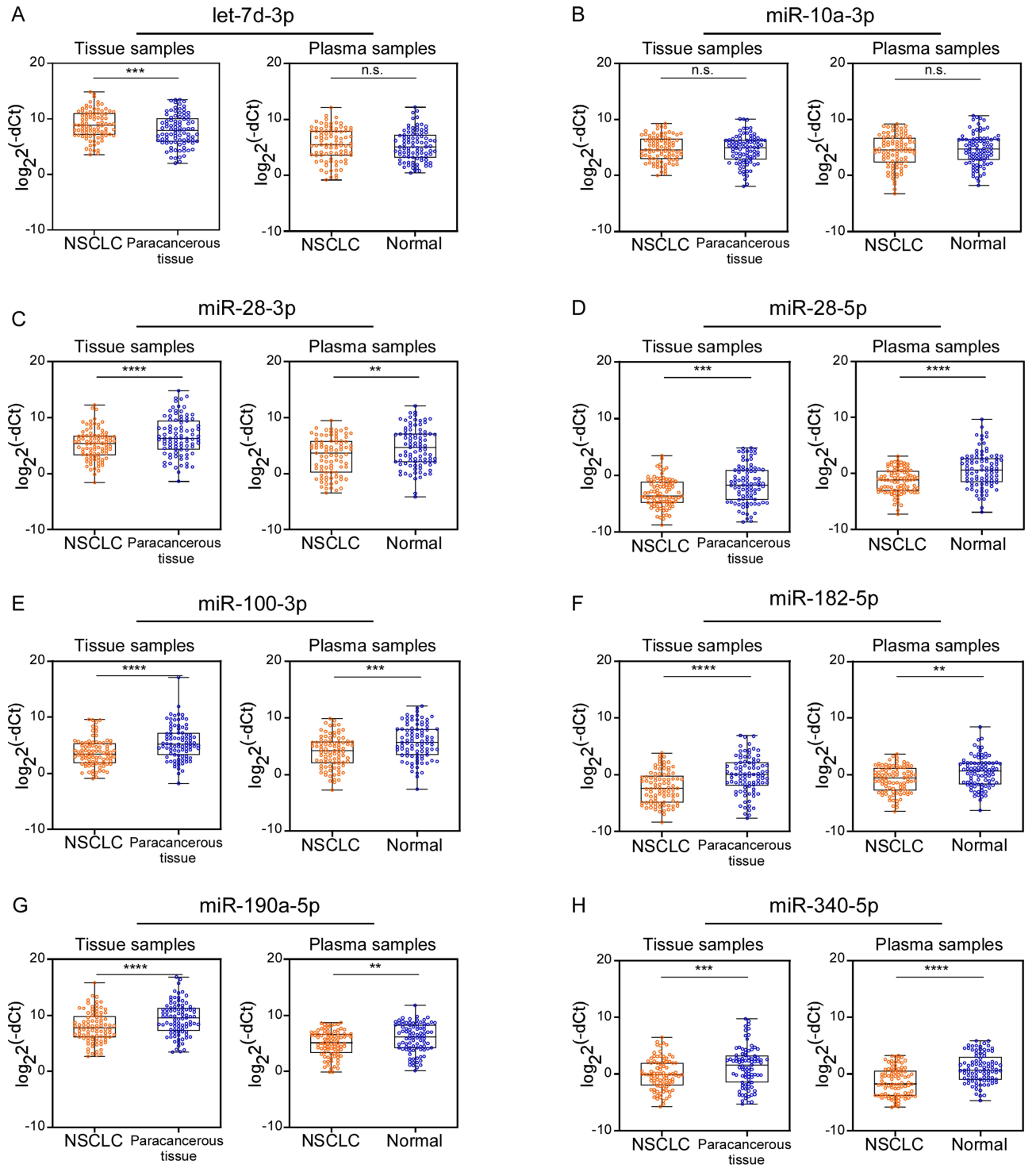

Figure 2 Relative expression of selected miRNAs in NSCLC tissue (n=89) and plasma (n=89) compared to paracancerous and normal samples. The expression levels of let-7d-3p (**A**), miR-10a-3p (**B**), miR-28-3p (**C**), miR-28-5p (**D**), miR-100-3p (**E**), miR-182-5p (**F**), miR-190a-5p (**G**), and miR-340-5p (**H**) were normalized to the housekeeping gene RNU6B and determined by the $2^{-\Delta Ct}$ method. Wilcoxon and Mann–Whitney tests were used to evaluate statistically significant differences. Whiskers of the boxplot denote the nonoutlier range.

Notes: ** indicates $p < 0.01$, *** indicates $p < 0.001$, **** indicates $p < 0.0001$, n.s. indicates non-significant.

41.6–61.4) in tumor and 48.2 months (95% CI: 37.7–58.7) in plasma; for miR-28-3p, 50.8 months (95% CI: 40.8–60.8) in tumor and 46.4 months (95% CI: 37.2–55.7) in plasma; for miR-28-5p, 52.3 months (95% CI: 42.2–62.3) in tumor and 50.9 months (95% CI: 41.1–60.9) in plasma; for miR-100-3p, 46.2 months (95% CI: 37.3–55.1) in tumor and 50.0 months (95% CI: 40.8–59.3) in plasma; for miR-182-5p, 51.0 months (95% CI: 41.4–60.7) in tumor and 51.4 months (95% CI: 41.4–61.4) in plasma; for miR-190a-5p, 47.6 months (95% CI: 37.7–57.4) in tumor and 51.4 months (95% CI: 41.0–61.9) in plasma; and for miR-340-5p, 47.7 months (95% CI: 37.9–57.6) in tumor and 49.1 months (95% CI: 38.9–59.3) in plasma. However, there were no statistically significant results between selected miRNAs expression and NSCLC patients OS rates (Figures S1 and S2). The analysis of OS in NSCLC patients, stratified by specific miRNA expression levels in tumor tissue and plasma, reveals nuanced variations in survival rates for individual miRNAs. Despite these variations, the absence of statistically significant results between miRNA expression levels and NSCLC patients' OS rates suggests that the examined miRNAs may not be robust predictors of overall survival in this context. Further research and exploration are warranted to better understand the potential prognostic implications and clinical significance of these miRNAs in NSCLC OS rates.

Also, the mean PFS for all NSCLC patients was 57.8 months (95% CI: 49.3–66.4), and when stratified by high expression levels of specific microRNAs (miRNAs) in tumor tissue and plasma, the PFS rates varied as follows: for let-7d-3p, 58.0 months (95% CI: 45.6–70.3) in tumor and 61.2 months (95% CI: 49.4–73.1) in plasma; for miR-10a-3p, 60.8 months (95% CI: 48.7–72.9) in tumor and 67.8 months (95% CI: 56.3–79.3) in plasma; for miR-28-3p, 56.1 months (95% CI: 44.0–68.2) in tumor and 57.2 months (95% CI: 45.2–69.1) in plasma; for miR-28-5p, 52.8 months (95% CI: 41.1–64.6) in tumor and 59.9 months (95% CI: 48.0–71.7) in plasma; for miR-100-3p, 52.1 months (95% CI: 40.1–64.2) in tumor and 56.9 months (95% CI: 44.7–69.1) in plasma; for miR-182-5p, 55.5 months (95% CI: 43.2–67.8) in tumor and 55.7 months (95% CI: 43.4–67.9) in plasma; for miR-190a-5p, 55.6 months (95% CI: 43.6–67.5) in tumor and 63.9 months (95% CI: 51.9–75.9) in plasma; and for miR-340-5p, 55.8 months (95% CI: 43.9–67.7) in tumor and 60.5 months (95% CI: 48.5–72.5) in plasma. Overall, data analysis demonstrated that patients with high miR-10a-3p expression in plasma (Figure 3B, p=0.009) had longer PFS rates than those with low miRNA expression. No other statistically significant results were identified (Figure 3A, C–H). Kaplan Meier curves of PFS according to selected miRNAs expression in NSCLC tumor tissue are presented in Figure S3.

Further analysis was done to identify the prognostic factors for OS and PFS of NSCLC patients. Univariate and multivariate Cox regression analysis was conducted on both tissue and plasma samples. Based on the univariate Cox regression analysis, lymph node status was identified as a prognostic factor for OS and PFS for NCSLC patients (respectively HR: 2.4, 95% CI: 1.0–4.6, p=0.006; HR: 2.8, 95% CI: 1.4–5.5, p=0.003). Moreover, NSCLC patients' gender and tumor pathological stage also are statistically significant variables for NSCLC patients' PFS rates (respectively HR: 2.0, 95% CI: 1.0–4.1, p=0.047; HR: 2.5, 95% CI: 1.4–4.6, p=0.003). Finally, our results suggest that in NSCLC patient plasma samples circulating miR-10a-3p can be evaluated as a significant independent prognostic factor for progression-free survival (HR: 0.5, 95% CI: 0.3–0.9, p=0.029; Figure 4). Full Univariate and Multivariate Cox regression analysis of prognostic factors for NSCLC patients OS and PFS in tumor tissue and plasma is presented in Tables S5–S8.

Discussion

A growing number of studies focused on miRNA expression in NSCLC show significant promise in the advancement of cancer diagnosis and therapy. miRNAs possess the capacity to influence crucial signaling pathways in NSCLC, potentially enhancing the cytotoxicity of anti-cancer drugs and/or preventing drug resistance. This, in turn, can have an impact on the effectiveness of current treatment approaches and patients' survival rates.[34] Cell culture is a highly valuable tool employed in both fundamental and applied cancer research. For a sustained period, 2D cell cultures have served as in vitro models for investigating how cells respond to various stimuli, including physical and chemical signals. While these methods have been widely accepted and have advanced our comprehension of cell behavior, mounting evidence suggests that, in certain situations, the outcomes in 2D systems may diverge significantly from in vivo responses. Moreover, crucial aspects of cancer cell characteristics may be insufficiently represented in 2D cultures.[35] Cells cultivated in monolayers exhibit distinct cellular and extracellular interactions, resulting in modified morphologies,

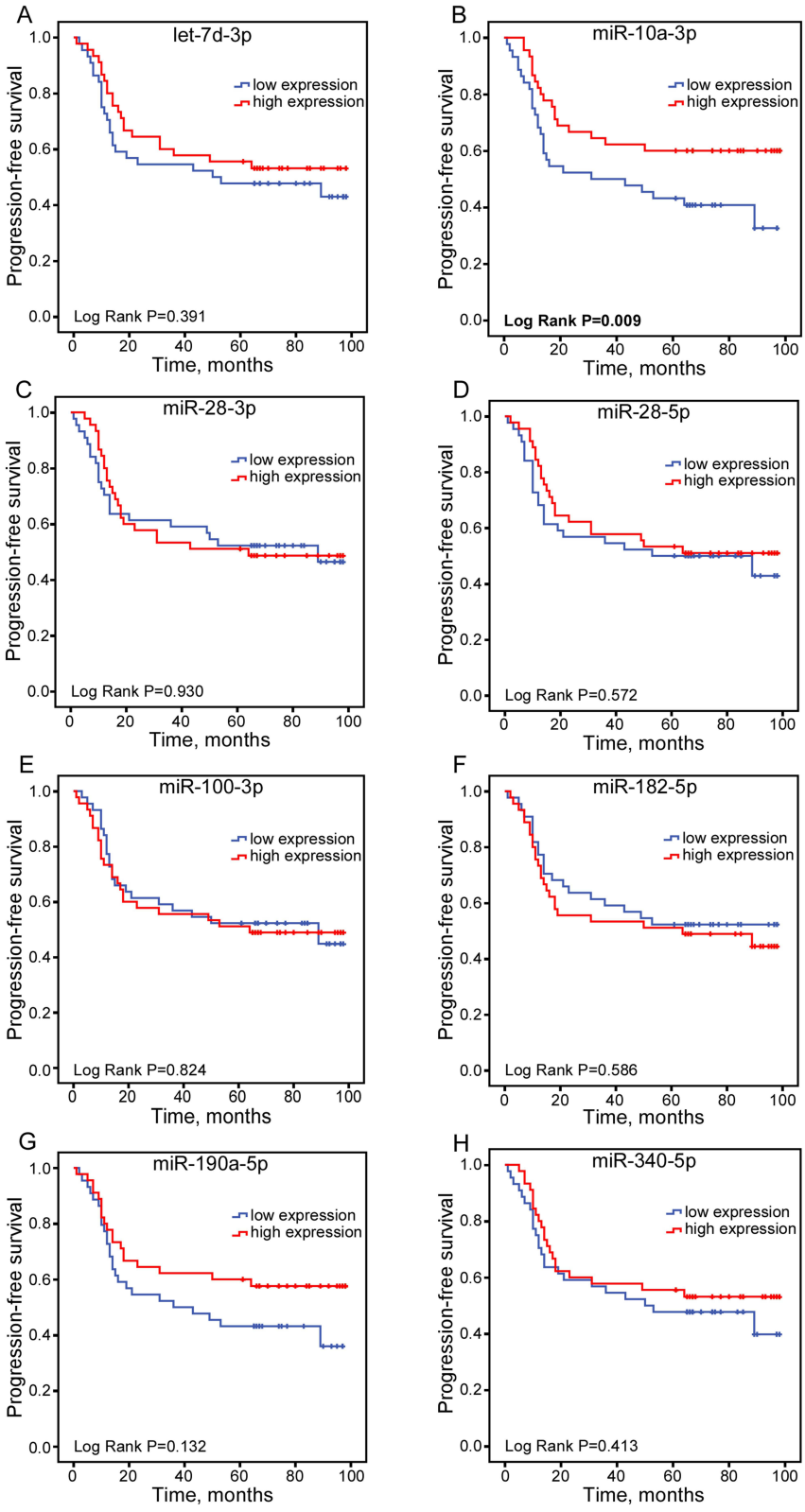

Figure 3 Kaplan-Meier curves illustrating PFS based on the expression of selected miRNAs in NSCLC plasma samples (n=89). Patients were categorized into high and low expression cohorts based on the median value of let-7d-3p (**A**), miR-10a-3p (**B**), miR-28-3p (**C**), miR-28-5p (**D**), miR-100-3p (**E**), miR-182-5p (**F**), miR-190a-5p (**G**), and miR-340-5p (**H**). The comparison between groups was conducted using the Log rank test, with corresponding p-values displayed. The bold text represents the statistically significant results ($p<0.05$).

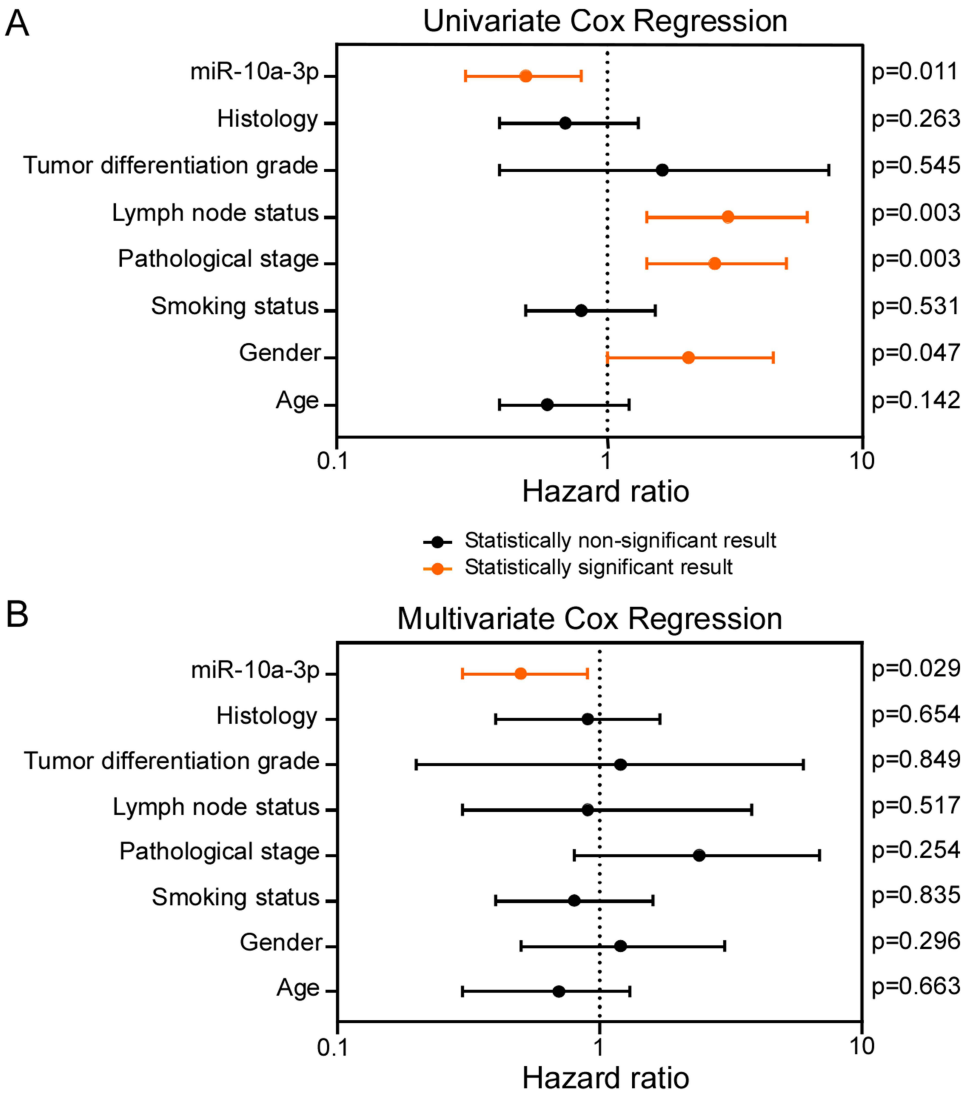

Figure 4 A forest plot of prognostic factors for NSCLC patients' PFS in plasma (n=89). A forest plot showing the hazard ratio and 95% confidence intervals associated with Univariate (**A**) and Multivariate (**B**) Cox Regression analysis of prognostic factors for NSCLC patients' PFS in plasma samples. Circles represent the hazard ratio, and the horizontal bars extend from the lower limit to the upper limit of the 95% confidence interval of the hazard ratio estimate. Horizontal bars colored in orange represent the statistically significant results ($p<0.05$), horizontal bars colored in black represent the statistically non-significant results ($p>0.05$).

genetic expression levels, treatment responses, and compromised access to metabolites and extracellular signals. To address this limitation, innovative 3D cell cultures are being developed to replicate in vivo conditions more accurately.[36] Key attributes of the 3D cell culture model include cell-to-cell and/or cell-to-ECM interactions and paracrine signaling facilitated by the diffusion of cellular secretions – features absent in conventional 2D cell culture. Consequently, the 3D cell culture model is anticipated to evolve into a refined and effective biotechnological system for investigating human diseases.[37] Therefore, NSCLC 3D cell culture models might play a crucial role in the exploration of novel clinically relevant biomarkers.

The present study demonstrated the connection of deregulation of let-7d-3p, miR-10a-3p, miR-28-3p, miR-28-5p, miR-100-3p, miR-182-5p, miR-190a-5p, and miR-340-5p with relative aggressiveness of NSCLC cell lines grown in the 3D culture system. Although all the cell lines used originate from lung tumor, they are sourced from different tissue types and exhibit substantially different genomic alterations. For instance, H23 and A549 lines are derived from tumor tissue, whereas Calu-1 and H1299 are derived from lung cancer metastasis. In addition, these cell lines display different karyotypic profiles. For example, A549 and Calu-1 cell lines are reported to be hypotriploid. The cell lines also vary in

driver gene mutations with the most common mutations found in TP53 (H23, Calu-1, H1299), KRAS (H23, Calu-1, A549) and SMARCA4 (H23, A549, H1299) genes. Therefore, differences in miRNA expression profiles between these cell lines might be inherent.[38,39] Our earlier findings indicate the significance of employing 3D cell culture as an essential experimental strategy to clarify the regulation of genes and miRNA involved in molecular processes influenced by the tumor microenvironment in vivo.[40] We demonstrated that colorectal cancer cells (CRC) cultivated in 3D culture showed different gene expression profiles in contrast to cells cultured in 2D. This included an increase in the expression of markers associated with cancer stem cells and endothelial-mesenchymal transition.[41] Moreover, the application of radiation treatment led to distinct genome-wide gene expression patterns in CRC cultivated in 3D culture conditions compared to those in 2D.[42] Through the application of a 3D cell culture technique, it was determined that miR-142-5p holds promise as a theranostic biomarker for Neoadjuvant Long-Course rectal cancer therapy.[43] Therefore, we hypothesized that miRNA expression patterns in NSCLC cells with different aggressiveness status grown in 3D cell culture conditions could potentially resemble the clinical tumor tissue significance and could be employed for the discovery of novel non-invasive biomarkers for NSCLC.

The identification of miRNAs that actively regulate tumorigenesis offers potential predictive and prognostic biomarkers for NSCLC patients.[44] To address this question, we further validated the expression of eight selected miRNAs (let-7d-3p, miR-10a-3p, miR-28-3p, miR-28-5p, miR-100-3p, miR-182-5p, miR-190a-5p, and miR-340-5p) in eighty-nine NSCLC patients tumor tissue and plasma samples. The expression analysis of selected miRNAs for the first time demonstrates that in NSCLC patient plasma samples circulating miR-10a-3p is a significantly independent prognostic factor for progression-free survival. The identification of circulating miR-10a-3p as a clinically relevant biomarker holds considerable promise for its utility in personalized medicine and disease progression monitoring. The integration of miR-10a-3p assessment into personalized treatment strategies could enable more precise and tailored interventions, optimizing therapeutic outcomes for individual patients.[45] Furthermore, the incorporation of miR-10a-3p into routine disease monitoring protocols not only offers a non-invasive and accessible means to detect potential relapses but also provides a valuable avenue for guiding timely therapeutic adjustments, emphasizing the translational potential of miR-10a-3p as a biomarker in advancing patient care within the context of targeted interventions and precision medicine approaches.[46,47]

The miR-10 family comprises two main members: miR-10a, located on chromosome 17, and miR-10b, located on chromosome 2. The nucleotide sequences of these two miRNAs exhibit a high degree of resemblance, suggesting potential similarities in their biological functions.[48] A precursor miRNA has two arms: miR-5p and miR-3p. Depending on the tissue or cell types, one of the two or both arms can be abundant.[49] Understanding the tumor-suppressive role of miR-10a-3p not only sheds light on the observed outcomes but also underscores its clinical significance, suggesting a promising application for individualized therapeutic interventions and enhanced disease management strategies.[50] Based on our miRNA target analysis using the KEGG pathway, we found that the targets of miR-10a-3p play crucial roles in regulating cell cycle, cellular senescence, and pathways associated with cancer. One of its target genes is *VEGFA*, known for its role in angiogenesis, a crucial process in tumor development, facilitating the transport of nutrients required for tumor growth.[51] Another target gene, *CCND1* encodes the cyclin D1 protein, contributing to cell cycle progression by inducing G1-S transition through activation of cyclin-dependent kinases, Cdk4 and Cdk6. Increased *CCND1* expression has been associated with high histopathological grade, elevated Ki-67 levels, and an increased mitotic count in breast cancer samples.[52] One crucial factor to consider in lung cancer is patients' smoking history. Cigarette smoke, a complex mixture of chemicals, significantly alters gene expression, including miRNA profiles that may contribute to tumor progression and metastasis. For instance, smoke upregulates TGF-β1, which subsequently inhibits CDK4 and cyclin D1 – a potential target of miR-10a, leading to cell cycle arrest in alveolar epithelial cells.[53] Alterations in miRNA expression caused by smoking can create a microenvironment that promotes tumor cell invasion and migration.[54] Studies have shown that miR-10a demonstrates remarkable efficacy in suppressing the proliferation and migration of breast cancer cells, while also promoting apoptosis. This is achieved through its regulation of the PI3K/Akt/mTOR signaling pathway, which is a crucial regulator in various cellular processes such as survival, proliferation, migration, metabolism, and apoptosis.[55] Additionally, by participating in the post-transcriptional regulation of *BCL6*, an important transcriptional repressor in B-cell differentiation implicated in apoptosis, cell cycle control, survival, and inflammatory responses, miR-10a-3p potentially impacts various cellular processes, underscoring its importance in cancer biology.[56] Results from other

research groups have shown that high miR-10a-3p expression is associated with a higher probability of death compared to low miR-10a-3p expression, and it can be used as an independent risk factor for prognosis in patients with severe pneumonia.[57] Additionally, miR-10a is significantly upregulated in lung squamous cell carcinoma compared to solitary metastatic lung tumors. Its expression in serum extracellular vesicles presents a promising noninvasive tool for the differential diagnosis of lung squamous cell carcinoma and solitary metastatic lung tumors.[58] Moreover, Wang et al demonstrated that exosomal miR-10a, derived from colorectal cancer cells, decreases the proliferative and migratory abilities of primary normal human lung fibroblasts, and reduces the expression levels of IL-6, IL-8, and IL-1β in these cells, offering insights into the phenotypic alterations and mechanisms underlying lung metastasis in colorectal cancer.[59] Finally, high miR-10a expression has been associated with tumor node and lymph node metastasis, and through targeting *PTEN*, it promotes NSCLC cell proliferation, migration, and invasion in vitro.[60] Thus, the multifaceted regulatory role of miR-10a-3p underscores its potential as a significant player in personalized therapeutic strategies and comprehensive disease management approaches.

Our study has some limitations. To begin with, artificial cell lines may not entirely reflect the complexity of in vivo biological systems, potentially leading to variations in responses and outcomes.[61] Genetic instability that can occur during prolonged cell culturing, phenotypic variability, and the lack of complex in vivo microenvironment are additional challenges that may influence the reliability and reproducibility of experimental results.[62] Moreover, the utilization of 3D cell cultures in this study introduces specific limitations. The homogeneity of cells in 3D cultures, the development of gradients in nutrients and oxygen, and the absence of an immune system, which holds significance in the physiological environment, may affect the consistency and replicability of results.[63] Therefore, cancer organoids could better replicate the complexity of the tumor microenvironment, including cellular heterogeneity, extracellular matrix interactions, and physiological gradients.[64] An additional limitation arises from the discordance in miRNA expression profiles between NSCLC cells and tissue/plasma samples. It may be potentially attributed to the intricate tumor heterogeneity characterizing varied cellular compositions and microenvironmental intricacies.[65] Finally, the small sample size could introduce inherent limitations which could lead to the increased chance of overlooking significant tumor associated effects (eg tumor pathological stage) or relationships of selected miRNAs. Therefore, potential avenues for future research with larger, independent sample sizes are needed to validate and extend our present results. Despite these limitations, the current study deployed 3D cell culture model to investigate miRNA expression levels in lung cancer cells with varying aggressiveness status and explored the relationship between selected miRNAs and patient survival rates, providing valuable insights into the clinical basis for the prognosis of NSCLC.

Conclusions

Our screening of miRNA expression patterns in NSCLC cells grown in 3D cell culture revealed that, out of the 8 miRNAs investigated (let-7d-3p, miR-10a-3p, miR-28-3p, miR-28-5p, miR-100-3p, miR-182-5p, miR-190a-5p, and miR-340-5p), only circulating miR-10a-3p demonstrated significant potential as a novel non-invasive biomarker for reflecting the short-term prognosis of NSCLC patients. Further investigations in diverse patient populations are required to verify the potential clinical application of miR-10a-3p.

Abbreviations

NSCLC, non-small cell lung cancer; OS, overall survival; PFS, progression-free survival; N0, no regional lymph nodes involvement; N1, involvement of ipsilateral peribronchial and/or ipsilateral hilar lymph nodes (includes direct extension to intrapulmonary nodes); N2, involvement of the ipsilateral mediastinal and/or subcarinal lymph nodes; G1, well differentiated tumor; G2, moderately differentiated tumor; G3, poorly differentiated tumor; ADC, adenocarcinoma; SCC, squamous cell carcinoma; HR, Hazard ratio; CI, confidence interval; Ref., reference group; FDR, false discovery rate; NGS, Next Generation Sequencing.

Data Sharing Statement

The datasets used and/or analyzed during the current study are available from the corresponding author upon reasonable request.

Ethics Approval and Consent to Participate

We confirm that the study complies with the Declaration of Helsinki, and is approved by the Vilnius Regional Bioethics Committee (No. 158200-05-455-141). All patients have signed informed consents. We confirm that all methods were performed in accordance with the relevant guidelines and regulations.

Acknowledgments

The authors are grateful to the patients who participated in this study.

Author Contributions

All authors made a significant contribution to the work reported, whether that is in the conception, study design, execution, acquisition of data, analysis and interpretation, or in all these areas; took part in drafting, revising or critically reviewing the article; gave final approval of the version to be published; have agreed on the journal to which the article has been submitted; and agree to be accountable for all aspects of the work.

Funding

This research was supported funded by the Ph.D. studies Grant to JS, Grant No. S-LB-19-7 from the Research Council of Lithuania, grant No. MTEP-2 from the National cancer institute (Lithuania).

Disclosure

The authors confirm that there are no known conflicts of interest associated with this publication and the financial support received has no influence to its outcome.

References

1. Phillips I, Stares M, Allan L, Sayers J, Skipworth R, Laird B. Optimising outcomes in non small cell lung cancer: targeting cancer cachexia. *Front Biosci*. 2022;27(4):129.
2. Long L, Zhang X, Bai J, Li Y, Wang X, Zhou Y. Tissue-specific and exosomal miRNAs in lung cancer radiotherapy: from regulatory mechanisms to clinical implications. *Cancer Manag Res*. 2019;11:4413–4424. doi:10.2147/CMAR.S198966
3. Pei Q, Luo Y, Chen Y, Li J, Xie D, Ye T. Artificial intelligence in clinical applications for lung cancer: diagnosis, treatment and prognosis. *Clin Chem Lab Med*. 2022;60(12):1974–1983. doi:10.1515/cclm-2022-0291
4. Li J, Zhang Q, Jiang D, Shao J, Li W, Wang C. CircRNAs in lung cancer- role and clinical application. *Cancer Lett*. 2022;544:215810. doi:10.1016/j.canlet.2022.215810
5. Markou A, Lianidou E, Georgoulias V. Metastasis-related miRNAs: a new way to differentiate patients with higher risk? *Future Oncol*. 2015;11(3):365–367. doi:10.2217/fon.14.294
6. Cuttano R, Afanga MK, Bianchi F. MicroRNAs and drug resistance in non-small cell lung cancer: where are we now and where are we going. *Cancers*. 2022;14(23):5731. doi:10.3390/cancers14235731
7. Liao Y, Wu X, Wu M, Fang Y, Li J, Tang W. Non-coding RNAs in lung cancer: emerging regulators of angiogenesis. *J Transl Med*. 2022;20(1):349. doi:10.1186/s12967-022-03553-x
8. Wani JA, Majid S, Imtiyaz Z, et al. MiRNAs in lung cancer: diagnostic, prognostic, and therapeutic potential. *Diagnostics*. 2022;12(7):1610. doi:10.3390/diagnostics12071610
9. Du M, Wang J, Chen H, et al. MicroRNA-200a suppresses migration and invasion and enhances the radiosensitivity of NSCLC cells by inhibiting the HGF/c-Met signaling pathway. *Oncol Rep*. 2019;41(3):1497–1508. doi:10.3892/or.2018.6925
10. Shen J, Liu Z, Todd NW, et al. Diagnosis of lung cancer in individuals with solitary pulmonary nodules by plasma microRNA biomarkers. *BMC Cancer*. 2011;11(1):374. doi:10.1186/1471-2407-11-374
11. Shen J, Todd NW, Zhang H, et al. Plasma microRNAs as potential biomarkers for non-small-cell lung cancer. *Lab Invest*. 2011;91(4):579–587. doi:10.1038/labinvest.2010.194
12. Lebanony D, Benjamin H, Gilad S, et al. Diagnostic assay based on hsa-miR-205 expression distinguishes squamous from nonsquamous non-small-cell lung carcinoma. *J Clin Oncol*. 2009;27(12):2030–2037. doi:10.1200/JCO.2008.19.4134
13. Hu Z, Chen X, Zhao Y, et al. Serum microRNA signatures identified in a genome-wide serum microRNA expression profiling predict survival of non-small-cell lung cancer. *J Clin Oncol*. 2010;28(10):1721–1726. doi:10.1200/JCO.2009.24.9342
14. Xie Y, Todd NW, Liu Z, et al. Altered miRNA expression in sputum for diagnosis of non-small cell lung cancer. *Lung Cancer*. 2010;67(2):170–176. doi:10.1016/j.lungcan.2009.04.004
15. Xing L, Todd NW, Yu L, Fang H, Jiang F. Early detection of squamous cell lung cancer in sputum by a panel of microRNA markers. *Mod Pathol*. 2010;23(8):1157–1164. doi:10.1038/modpathol.2010.111
16. Liao J, Shen J, Leng Q, Qin M, Zhan M, Jiang F. MicroRNA-based biomarkers for diagnosis of non-small cell lung cancer (NSCLC). *Thorac Cancer*. 2020;11(3):762–768. doi:10.1111/1759-7714.13337

17. Cheng H, Yang X, Si H, et al. Genomic and transcriptomic characterization links cell lines with aggressive head and neck cancers. *Cell Rep*. 2018;25(5):1332–1345.e5. doi:10.1016/j.celrep.2018.10.007
18. Leung EL, Fiscus RR, Tung JW, et al. Non-small cell lung cancer cells expressing CD44 are enriched for stem cell-like properties. *PLoS One*. 2010;5(11):e14062. doi:10.1371/journal.pone.0014062
19. Yang SY, Li Y, An GS, Ni JH, Jia HT, Li SY. DNA damage-response pathway heterogeneity of human lung cancer A549 and H1299 cells determines sensitivity to 8-chloro-adenosine. *Int J Mol Sci*. 2018;19(6):E1587. doi:10.3390/ijms19061587
20. Ceppi P, Mudduluru G, Kumarswamy R, et al. Loss of miR-200c expression induces an aggressive, invasive, and chemoresistant phenotype in non-small cell lung cancer. *Mol Cancer Res*. 2010;8(9):1207–1216. doi:10.1158/1541-7786.MCR-10-0052
21. Bol GM, Vesuna F, Xie M, et al. Targeting DDX3 with a small molecule inhibitor for lung cancer therapy. *EMBO Mol Med*. 2015;7(5):648–669. doi:10.15252/emmm.201404368
22. Guo L, Zhang K, Bing Z. Application of a co-expression network for the analysis of aggressive and non-aggressive breast cancer cell lines to predict the clinical outcome of patients. *Mol Med Rep*. 2017;16(6):7967–7978. doi:10.3892/mmr.2017.7608
23. Takagi A, Watanabe M, Ishii Y, et al. Three-dimensional cellular spheroid formation provides human prostate tumor cells with tissue-like features. *Anticancer Res*. 2007;27(1A):45–53.
24. Riedl A, Schlederer M, Pudelko K, et al. Comparison of cancer cells in 2D vs 3D culture reveals differences in AKT-mTOR-S6K signaling and drug responses. *J Cell Sci*. 2017;130(1):203–218. doi:10.1242/jcs.188102
25. Stankevicius V, Kunigenas L, Stankunas E, et al. The expression of cancer stem cell markers in human colorectal carcinoma cells in a microenvironment dependent manner. *Biochem Biophys Res Commun*. 2017;484(4):726–733. doi:10.1016/j.bbrc.2017.01.111
26. Andrews S. FastQC: a quality control tool for high throughput sequence data. Available From: http://www.bioinformatics.babraham.ac.uk/projects/fastqc. Accessed February 8, 2020.
27. Martin M. Cutadapt removes adapter sequences from high-throughput sequencing reads. *EBMnet J*. 2011;17.
28. Langmead B, Salzberg SL. Fast gapped-read alignment with Bowtie 2. *Nat Methods*. 2012;9(4):357–359. doi:10.1038/nmeth.1923
29. Kozomara A, Griffiths-Jones S. miRBase: annotating high confidence microRNAs using deep sequencing data. *Nucleic Acids Res*. 2014;42(D1):D68–D73. doi:10.1093/nar/gkt1181
30. Robinson MD, McCarthy DJ, Smyth GK. edgeR: a Bioconductor package for differential expression analysis of digital gene expression data. *Bioinformatics*. 2010;26(1):139–140. doi:10.1093/bioinformatics/btp616
31. Karagkouni D, Paraskevopoulou MD, Chatzopoulos S, et al. DIANA-TarBase v8: a decade-long collection of experimentally supported miRNA–gene interactions. *Nucleic Acids Res*. 2017:gkx1141.
32. Liao Y, Wang J, Jaehnig EJ, Shi Z, Zhang B. WebGestalt 2019: gene set analysis toolkit with revamped UIs and APIs. *Nucleic Acids Res*. 2019;47(W1):199–205. doi:10.1093/nar/gkz401
33. Schmittgen TD, Livak KJ. Analyzing real-time PCR data by the comparative C(T) method. *Nat Protoc*. 2008;3(6):1101–1108. doi:10.1038/nprot.2008.73
34. Yang H, Liu Y, Chen L, et al. MiRNA-based therapies for lung cancer: opportunities and challenges? *Biomolecules*. 2023;13(6):877. doi:10.3390/biom13060877
35. Duval K, Grover H, Han LH, et al. Modeling physiological events in 2D vs. 3D cell culture. *Physiology*. 2017;32(4):266–277. doi:10.1152/physiol.00036.2016
36. El Feky SE, Ghany Megahed MA, El Moneim NA A, Zaher ER, Khamis SA, Ali LMA. Cytotoxic, chemosensitizing and radiosensitizing effects of curcumin based on thioredoxin system inhibition in breast cancer cells: 2D vs. 3D cell culture system. *Exp Ther Med*. 2021;21(5):506. doi:10.3892/etm.2021.9937
37. Lee SY, Koo IS, Hwang HJ, Lee DW. In Vitro three-dimensional (3D) cell culture tools for spheroid and organoid models. *SLAS Discov*. 2023;28(4):119–137. doi:10.1016/j.slasd.2023.03.006
38. Cosmic. COSMIC - Catalogue of Somatic Mutations in Cancer. Available from: https://cancer.sanger.ac.uk/cosmic. Accessed August 13, 2024.
39. ATCC: the Global Bioresource Center. Available from: https://www.atcc.org/. Accessed August 13, 2024.
40. Stankevicius V, Vasauskas G, Bulotiene D, et al. Gene and miRNA expression signature of Lewis lung carcinoma LLC1 cells in extracellular matrix enriched microenvironment. *BMC Cancer*. 2016;16(1):789. doi:10.1186/s12885-016-2825-9
41. Stankevicius V, Vasauskas G, Noreikiene R, Kuodyte K, Valius M, Suziedelis K. Extracellular matrix-dependent pathways in colorectal cancer cell lines reveal potential targets for anticancer therapies. *Anticancer Res*. 2016;36(9):4559–4567. doi:10.21873/anticanres.11004
42. Stankevicius V, Vasauskas G, Rynkeviciene R, et al. Microenvironment and dose-delivery-dependent response after exposure to ionizing radiation in human colorectal cancer cell lines. *Radiat Res*. 2017;188(3):291–302. doi:10.1667/RR14658.1
43. Kunigenas L, Stankevicius V, Dulskas A, et al. 3D cell culture-based global miRNA expression analysis reveals miR-142-5p as a theranostic biomarker of rectal cancer following neoadjuvant long-course treatment. *Biomolecules*. 2020;10(4):613. doi:10.3390/biom10040613
44. Szczyrek M, Bitkowska P, Jutrzenka M, Milanowski J. The role of the selected miRNAs as diagnostic, predictive and prognostic markers in non-small-cell lung cancer. *J Pers Med*. 2022;12(8):1227. doi:10.3390/jpm12081227
45. Mathur S, Sutton J. Personalized medicine could transform healthcare. *Biomed Rep*. 2017;7(1):3–5. doi:10.3892/br.2017.922
46. Lokshin A, Bast RC, Rodland K. Circulating cancer biomarkers. *Cancers*. 2021;13(4):802. doi:10.3390/cancers13040802
47. Wilson JL, Altman RB. Biomarkers: delivering on the expectation of molecularly driven, quantitative health. *Exp Biol Med*. 2018;243(3):313–322. doi:10.1177/1535370217744775
48. Gao S, Liu S, Wei W, Qi Y, Meng F. Advances in targeting of miR-10-associated lncRNAs/circRNAs for the management of cancer (Review). *Oncol Lett*. 2023;25(3):89. doi:10.3892/ol.2023.13675
49. Mitra R, Lin CC, Eischen CM, Bandyopadhyay S, Zhao Z. Concordant dysregulation of miR-5p and miR-3p arms of the same precursor microRNA may be a mechanism in inducing cell proliferation and tumorigenesis: a lung cancer study. *RNA*. 2015;21(6):1055–1065. doi:10.1261/rna.048132.114
50. Chehelgerdi M, Chehelgerdi M, Allela OQB, et al. Progressing nanotechnology to improve targeted cancer treatment: overcoming hurdles in its clinical implementation. *Mol Cancer*. 2023;22(1):169. doi:10.1186/s12943-023-01865-0
51. Cuzziol CI, Castanhole-Nunes MMU, Pavarino ÉC, Goloni-Bertollo EM. MicroRNAs as regulators of VEGFA and NFE2L2 in cancer. *Gene*. 2020;759:144994. doi:10.1016/j.gene.2020.144994

52. Valla M, Klæstad E, Ytterhus B, Bofin AM. CCND1 amplification in breast cancer -associations with proliferation, histopathological grade, molecular subtype and prognosis. *J Mammary Gland Biol Neoplasia*. 2022;27(1):67–77. doi:10.1007/s10911-022-09516-8
53. Chai XM, Li YL, Chen H, Guo SL, Shui LL, Chen YJ. Cigarette smoke extract alters the cell cycle via the phospholipid transfer protein/transforming growth factor-β1/CyclinD1/CDK4 pathway. *Eur J Pharmacol*. 2016;786:85–93. doi:10.1016/j.ejphar.2016.05.037
54. Pezzuto A, Citarella F, Croghan I, Tonini G. The effects of cigarette smoking extracts on cell cycle and tumor spread: novel evidence. *Future Sci OA*. 2019;5(5):FSO394. doi:10.2144/fsoa-2019-0017
55. Ke K, Lou T. MicroRNA-10a suppresses breast cancer progression via PI3K/Akt/mTOR pathway. *Oncol Lett*. 2017;14(5):5994–6000. doi:10.3892/ol.2017.6930
56. Fan Q, Meng X, Liang H, et al. miR-10a inhibits cell proliferation and promotes cell apoptosis by targeting BCL6 in diffuse large B-cell lymphoma. *Protein Cell*. 2016;7(12):899–912. doi:10.1007/s13238-016-0316-z
57. Xie J, Li Y, Wang M, He W, Zhao X. Diagnostic and prognostic value of dysregulated miR-10a-3p in patients with severe pneumonia. *J Inflamm Res*. 2022;15:6097–6104. doi:10.2147/JIR.S380818
58. Shimada Y, Matsubayashi J, Saito A, Ohira T, Kuroda M, Ikeda N. Small RNA sequencing to differentiate lung squamous cell carcinomas from metastatic lung tumors from head and neck cancers. *PLoS One*. 2021;16(3):e0248206. doi:10.1371/journal.pone.0248206
59. Wang J, Liu Y, Li Y, et al. Exosomal miR 10a derived from colorectal cancer cells suppresses migration of human lung fibroblasts, and expression of IL 6, IL 8 and IL 1β. *Mol Med Rep*. 2021;23(1):84. doi:10.3892/mmr.2020.11723
60. Yu T, Liu L, Li J, et al. MiRNA-10a is upregulated in NSCLC and may promote cancer by targeting PTEN. *Oncotarget*. 2015;6(30):30239–30250. doi:10.18632/oncotarget.4972
61. Haddad MJ, Sztupecki W, Delayre-Orthez C, et al. Complexification of in vitro models of intestinal barriers, a true challenge for a more accurate alternative approach. *Int J Mol Sci*. 2023;24(4):3595. doi:10.3390/ijms24043595
62. Mu P, Zhou S, Lv T, et al. Newly developed 3D in vitro models to study tumor-immune interaction. *J Exp Clin Cancer Res*. 2023;42(1):81. doi:10.1186/s13046-023-02653-w
63. Urzì O, Gasparro R, Costanzo E, et al. Three-dimensional cell cultures: the bridge between in vitro and in vivo models. *Int J Mol Sci*. 2023;24(15):12046. doi:10.3390/ijms241512046
64. El Harane S, Zidi B, El Harane N, Krause KH, Matthes T, Preynat-Seauve O. Cancer spheroids and organoids as novel tools for research and therapy: state of the art and challenges to guide precision medicine. *Cells*. 2023;12(7):1001. doi:10.3390/cells12071001
65. Vickman RE, Faget DV, Beachy P, et al. Deconstructing tumor heterogeneity: the stromal perspective. *Oncotarget*. 2020;11(40):3621–3632. doi:10.18632/oncotarget.27736